International Journal of Steel Structures
https://doi.org/10.1007/s13296-018-0049-3

Experimental Testing and Finite Element Modelling of Steel Columns Weakened to Facilitate Building Demolition

W. J. van Jaarsveldt[1] · R. S. Walls[1] · E. van der Klashorst[1]

Received: 12 September 2017 / Accepted: 3 March 2018

Abstract
Negligible research has been conducted to date on how to analyse weakened columns, thus safety risks are still involved when structures are weakened prior to demolition. There are various methods available for demolishing steel structures. One of the most effective methods that has been developed involves pre-cutting steel columns at a certain height, so that the least effort can be used to collapse the structure by means of pulling out some of the columns. This paper presents (a) an experimental setup developed to test the capacity of axially loaded weakened columns, which is used to (b) validate a finite element (FE) model. The two pre-cuts that are presented in this paper are (1) the double window cut and (2) the triangular window cut, which are both commonly used in industry. A column weakened with a double window cut or triangular window cut reduces the axial load capacity by up to 50 and 40%, respectively. The FE models developed predict the axial failure load of weakened columns for a double window cut and triangular window cut are generally within an accuracy of less than 8 and 10%, respectively. It is shown at higher slendernesses the influence of column cuts is less than would be intuitively expected because global buckling becomes dominant.

Keywords Demolition engineering · Steel columns · Failure load · Abaqus · Finite element analysis · Collapse

1 Introduction

In practice various methods are used to demolish structures, ranging from simple 'brute-force' type approaches, to highly technical progressive demolition techniques, such as outlined by the JISF (2015). Multiple codes of practice have been produced to assist contractors during demolition [e.g. HK Bldg. Dept. (2004), Indian Standard 4130 (2002)]. Demolition associations have been formed, such as in the UK, USA and EU, to try assist demolition contractors and regulate the industry. However, these guidelines, codes and organisations typically only provide construction related guidelines without giving information to assist structural engineers who have to ensure that structures remain safe during the demolition process.

Minimal research has been conducted and literature published up to this point on predicting the load capacity of weakened structures (van Jaarsveldt and Walls 2016). The techniques and analysis methods used in industry rely primarily on experience obtained from previous projects, and are less focused on strict theoretical principles, although some practitioners may use simplified design equations. It is necessary that sound engineering and scientific principles be applied to this problem to produce verifiable and safe design techniques. Furthermore, with safety requirements becoming much stricter worldwide, contractors may now be required to show by calculation that their procedures are safe, which currently cannot easily be done.

One of the most effective methods available for demolishing structures involves the pre-cutting of steel columns of a structure at a certain height, using different types of cuts. This weakens the columns of the structure so that the least effort can be used to demolish the structure by means of pulling out some of the columns or by using explosives (NDA 2014). The pre-cutting of the columns is done manually, which causes this method to have safety implications. If a structure has been weakened too much it could collapse during the weakening process (Walls 2017). Conversely, if a structure has not been weakened enough it will not collapse when required, leading to a partially collapsed structure, which is also a very dangerous scenario. This paper will

✉ R. S. Walls
rwalls@sun.ac.za

[1] Department of Civil Engineering, University of Stellenbosch, Stellenbosch, South Africa

Published online: 14 May 2018

focus on determining the capacity of weakened columns through experimental testing and finite element modelling.

2 Background

Steel structures are demolished for different reasons, such as: removing buildings that have been damaged by fire or other events, to make way for new developments, or because buildings are no longer safe to use (NDA 2014). The demolition video screen-shots in Fig. 1 illustrate a furnace structure that was demolished by Jet Demolition (Pty) Ltd. For a detailed description of the collapse mechanism refer to Walls (2017). The structure was weakened through applying pre-cuts to the columns and the beams, as shown in Fig. 1a. However, the furnace can be seen to remain in its original position, whilst demolition staff were operating in the area. The middle columns of the structure were then pulled out using steel cables as shown in Fig. 1b. This caused the structure to fail as seen in Fig. 1c. This process illustrates one of the current industry approaches used for the demolition of steel structures.

The cuts that have been investigated in this paper are shown in Fig. 2. The dimensions of the cuts presented in Fig. 2 are based upon those used in industry, although in theory an infinite number of configurations are possible

Fig. 1 Demolition of a furnace structure, with **a** showing where cuts were made, **b** the structure when columns were being pulled out, and **c** the collapse mechanism that resulted (Reproduced with permission from Walls 2017)

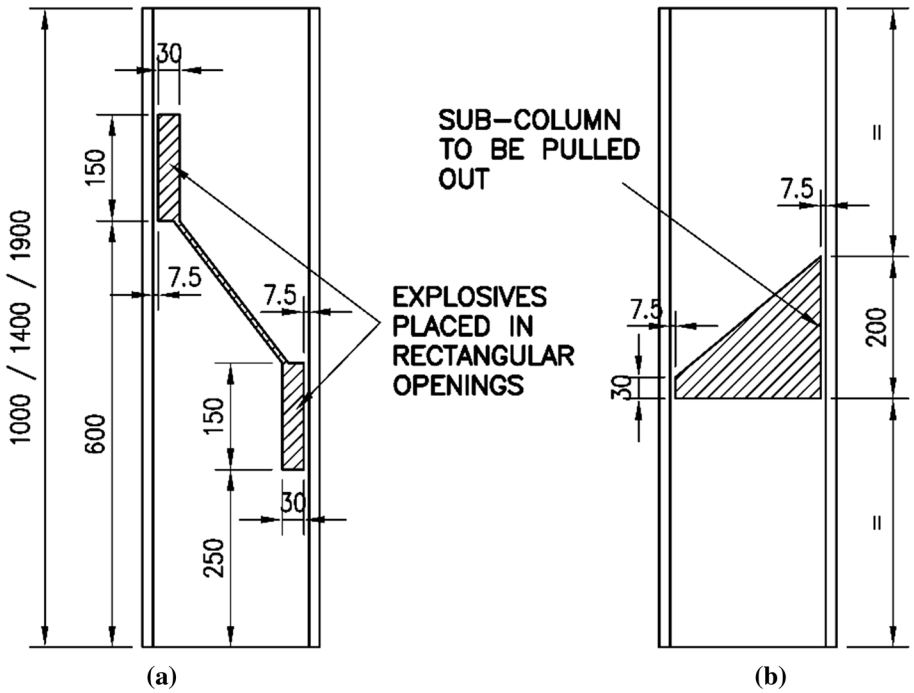

Fig. 2 Cuts commonly applied to steel columns in practice, showing **a** the double window cut (left), and **b** the triangular window cut (right)

(provided that they fit within the geometry of the section). In this paper the cut geometry between different size columns has been left constant to reduce the amount of variables, although it is important to understand the influence of this geometry. Section 5.5 provides an additional discussion regarding the influence of cut parameters.

The purpose of the double window cut is to weaken the column so that the least amount of explosives can be used to initiate the failure of a structure. The explosives are placed in the two rectangular windows. The explosives blow the flanges out, which causes the column to collapse approximately vertically downwards under the weight of the structure above. The triangular window cut is used in practice to weaken a column such that it will hinge in a particular direction when subjected to a lateral load, to ensure that collapse happens in a certain orientation. If a cut is made through the sub-column flange section shown, it allows demolition contractors to initiate collapse through applying a lateral load directly to the sub-column and pulling it out. Sub-columns are defined as small sections within a larger column adjacent to cuts, whose behaviour can be approximated as small individual column sections.

The work presented in this paper expands upon an initial investigation by van Jaarsveldt and Walls (2016) which has investigated a variety of weakening techniques. This work followed preliminary investigations by van Helsdingen (2012) at the University of Pretoria. From the detailed FE models and experimental testing conducted in this current investigation shortcomings in the initial work have been identified, such as modelling boundary conditions, the material properties specified, the preparation of the specimens and initial geometric imperfections used in the FE models. Further research investigating the influence of the shim techniques used during demolition, and the lateral forces required to initiate collapse have been conducted by Dunn (2015) and Mitchell (2016) as part of this overall research project. For more detailed information regarding results, test procedures and analysis models presented in this paper refer to the thesis of van Jaarsveldt (2016).

3 Experimental Design Overview

This section provides an overview of the experimental setup used to determine the capacity of weakened columns. Results are presented in Sect. 5, along with finite element predictions.

3.1 Research Philosophy

On demolition sites holes that are made in columns and beams are typically cut out using oxyacetylene torches ("flame torches"), which have a low level of accuracy and subject steel elements to high temperatures in the vicinity of the cut. Figure 3 presents cuts made in real columns by a demolition contractor and tested to failure (van Helsdingen 2012), with pictures showing the localised damage in the vicinity of cuts. Based on inspections conducted by the authors it is conservatively estimated that an additional 5–10 mm of material is lost from the edge of a cut, due to damage and temperature effects, and this distance will vary depending on the skill of the operator, the complexity of the opening being cut and the thickness of the steel plate being weakened. Further research is required to more accurately define this distance.

To provide a reproducible and controlled test environment the cuts tested in this work have been made using a manually operated milling drill bit and premade templates. Hence, the results predicted in this research will be for an "effective" cut size, which is accurate and regular. In a design scenario

Fig. 3 Cuts made in columns using an oxyacetylene torch, showing damage to steel in the vicinity of cuts (Reproduced with permission from van Helsdingen 2012)

the "effective" size of an opening, as considered here, would be calculated by taking actual opening sizes that demolition teams aim to make on site, and (1) increasing the dimensions by 5–10 mm all around to allow for material damage, and (2) potentially adding an additional 5–10 mm to allow for operator accuracy.

An additional challenge faced when defining design parameters is that in buildings being demolished columns will generally form part of a larger structure, and thus will typically have moment continuity at their top and bottom. However, to reduce the influence of unknown factors and create a system which can be accurately numerically modelled pin-ended conditions have been used in this work. In early research focussed on developing steel testing methodologies it was found by Estuar and Tall (1967) that using pin-ended columns avoids problems such as St. Venant end effects and allows for factors influencing column strength to be studied independently.

A further uncertainty associated with designing steelwork for demolition is that buildings being weakened are typically old and the grade of steel originally used is unknown. However, this can be addressed by doing tests on materials on sites.

3.2 Test Specimens

The length of the column samples tested were chosen so that a wider range of the slenderness spectrum could be investigated. The sections that were tested were an IPE160, IPE200, UC 152 × 152 × 23 and a UC 152 × 152 × 30, with properties as shown in Fig. 4. These sections have been selected to investigate how I-sections and H-sections with differing geometries and slenderness ratios respond if they have been weakened. Three lengths of each cross-section size were tested: (1) a 0.6 m stub column of the IPE 160 section (which was only done on the IPE 160 to ensure that local failure was considered), (2) a short stub column of 1.0 m in length that generally underwent local buckling, (3) a 1.4 m specimen, and (4) a 1.9 m more slender column, that generally underwent global buckling. The maximum length of the latter sample was influenced by the testing equipment available. A total of 39 specimens were tested and are reported on in this work.

3.3 Test Setup

The recommended end fixture to use, according to Tebedge et al. (1971) amongst others, is a relatively large hardened cylindrical surface bearing on a flat hardened steel surface. In this work a bridge bearing was used with an axial capacity of 2 MN, which was accurately machined to provide the cylindrical bearing surface. In the tests the columns were orientated such that they were pinned about their minor axes, facilitating global failure. Rotation was prevented about the strong axis. Since local sub-column buckling occurs about the strong axis, which is not significantly influenced by boundary conditions, this setup was deemed most suitable. For future tests a dome bearing could be considered. Examples of specimens tested and the setup used are shown in Fig. 5.

3.4 Preparation of the Specimens

It was assumed that after cuts 7.5 mm of the web would remain (i.e. 7.5 mm from the edge of the flange to the edge of the cut), due to a flame torch not being able to cut directly along the face of the flange. These cuts were applied to the columns through the use of a manually operated milling bit, as mentioned above. Although the use of the milling bit caused a small radius to develop in each of the corners of the cut, it was concluded from preliminary FE models that this would have a negligible influence on the axial load capacity. Figure 2 shows the dimensions of cuts made to samples, as previously discussed.

To measure initial imperfections a tensioned steel cable was fixed to the two ends of the column at the same offset distance through the use of a hook and eye turnbuckle (Estuar and Tall 1967). The cable was pre-stressed to ensure that no lateral deflection would occur during contact with the Digital Vernier Caliper. Three measurements were recorded about the minor axis of the section at constant intervals along the length of the column. The largest

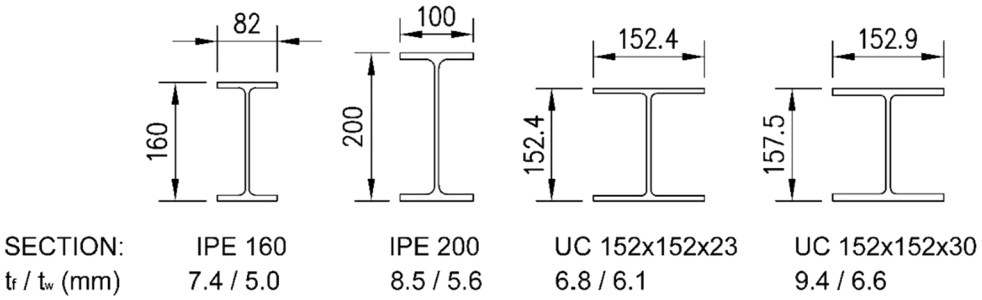

Fig. 4 Sections tested during experimental investigations, showing overall dimensions and the thickness of flanges (t_f) and webs (t_w)

(a) (b) (c)

Fig. 5 Test setup consisting of a 2 MN actuator with **a** a 1.4 m long sample with a double window cut, **b** a 1.4 m sample with a triangular window cut, and **c** the bearings used for testing

initial geometric imperfection measured was 1.1 mm at mid height for a 1.9 m long IPE 160 section.

Before testing each sample dimensions were measured to confirm actual sizes. Unfortunately the samples supplied had greater variations in cross-sectional properties than specified in SANS codes (South African codes of practice), resulting in some of the variations discussed in the results section. Flange and web thicknesses for the same member size varied by up to − 0.3 to + 0.7 mm, accounting some of the fluctuations in graphs observed. However, the measured dimensions were used in the FE models developed below, and are presented in the thesis of van Jaarsveldt (2016).

3.5 Tension Coupon Tests

Tensile tests were performed using a 250 kN Zwick machine (electro mechanical actuator) according to SANS 6892-1 (SABS 2010). Each section tested was cut from 13 m lengths obtained from local suppliers. The specimens for the tension coupon test were obtained from the flanges (4 coupons) and the web (3 coupons) for each of the 13 m lengths. The averages of the yield stress (f_y), ultimate stress (f_u) and the elastic modulus (E) were then taken respectively for the flange and the web, as presented in Table 1. Figure 6 illustrates the uniaxial tensile test stress–strain results obtained for the web and the flange of a UC 152 × 152 × 23 section. Material properties obtained were used in the FE models.

Table 1 Average yield stress, ultimate stress, elastic modulus and failure strains for the sections tested

Section	Specimen	Yield stress, f_y (MPa)	Ultimate stress, f_u (MPa)	E-modulus (GPa)	Strain at ultimate stress (–)	Failure strain (–)
IPE 200	Flange	400	549	200	0.14	0.25
	Web	433	556	211	0.14	0.24
UC 152×152×30	Flange	382	509	193	0.14	0.23
	Web	415	519	210	0.15	0.25
IPE 160	Flange	417	552	205	0.14	0.25
	Web	448	568	208	0.15	0.26
UC 152×152×23	Flange	431	543	207	0.16	0.29
	Web	401	553	200	0.14	0.23

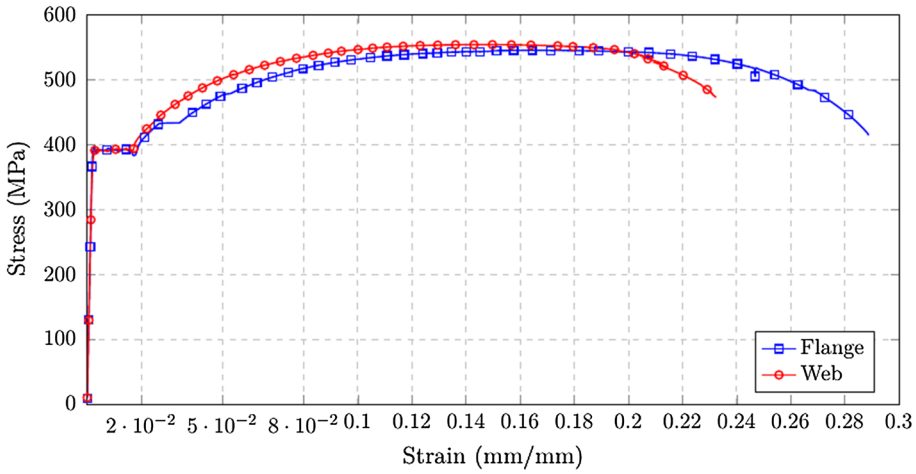

Fig. 6 Tensile test results of the web and flange for a UC 152 × 152 × 23 section

4 Finite Element Analysis

Finite element (FE) models were developed in order to study the behaviour of the weakened columns discussed in the previous section. The FE software package that was used for this purpose was Abaqus version 6.14-1 (Dassault Systèmes 2016).

4.1 Model Development

A FE model was set-up for each of the columns that were tested with the corresponding properties as described above. According to Avery and Mahendran (2000) satisfactory results are obtained using shell elements for the analysis of columns. A column can be defined as a thin-walled structure since the thickness of the column web and flanges are significantly smaller than the height of the web and the width of the flanges. For this paper the conventional S4R shell element was chosen, which is a 4-noded, double curved, shell element. This element accounts for finite membrane strains and arbitrary rotations making them suitable for large strain analysis. The S4R element uses a reduced integration scheme to form the element stiffness (Dassault Systèmes 2014).

4.2 Initial Geometric Imperfection and Buckling Modes

Every steel column has some form of initial geometric imperfection due to the production process, handling and installation of the column, building operations and load effects. This accounted for in design equations using partial factors and different buckling curves (BSI 2014; Chabrolin 2001). It must be understood that any building being demolished is typically old, has unknown steel properties, may have experienced damage over time, and the loading on elements is not accurately known. Hence, there are no guidelines available regarding how to determine a suitable initial geometric imperfection of an existing column in a building, although this influences finite element model predictions.

In this work the initial geometric imperfection along the length of a section was initially determined by measuring the column at multiple points, as mentioned above. However, the placing of samples in the testing rig, deformation of samples, imperfections in boundary conditions and machine tolerances leads to imperfections in excess of those measured for a sample in isolation. Hence, a model imperfection factor of Length/1000, according to SANS 2001:CS1 (SABS 2005), was selected.

According to Yuan (2004) there are random imperfections in steel columns and it is possible that these random imperfections may initiate buckling deformations. Nevertheless, the ultimate load capacity of a column is primarily determined by the buckling shape. For FE models the buckling shapes with the corresponding buckling loads were obtained from elastic buckling analyses. A nonlinear analysis was then used to obtain the full load–deflection response. Figure 7 illustrates the first three buckling shapes that were obtained for an IPE200 section with a double window cut. The first shape, Fig. 7a illustrates a local failure with the cut opening up and giving a buckling load of 647 kN. The second shape, Fig. 7b illustrates the column undergoing global buckling with a buckling load of 686 kN. Lastly, the third shape, Fig. 7c shows local failure in the web and flanges of the column giving a buckling load of 695 kN. All of these failure modes could potentially occur depending on the geometry, loading and boundary conditions of a section.

Figure 8 illustrates the first three buckling shapes that were obtained for an UC 152 × 152 × 30 section with a triangular window cut. The first shape, Fig. 8a illustrates a local failure of the sub-column with an associated buckling load of 988 kN. The second and third shapes, shown in Fig. 8b, c, illustrate warping of the flanges with buckling

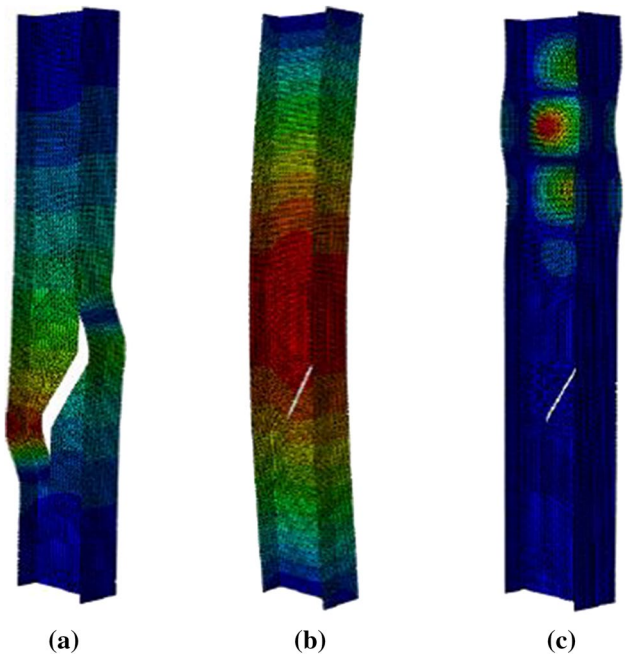

Fig. 7 Buckling shapes for an IPE 200 section with double window cut. **a** Sub-column buckling, **b** Lateral buckling, **c** Local distortional buckling

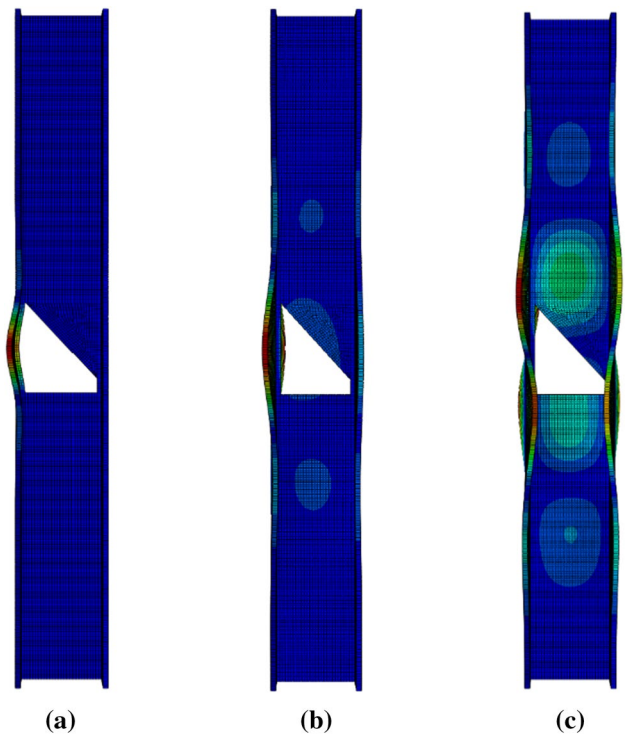

Fig. 8 Buckling shapes for a 152 × 152 × 30 section with triangular window cut. **a** Sub-column buckling, **b** Sub-column torsional buckling, **c** Sub-column torsional buckling second mode

loads of 1091 and 1100 kN, respectively. Global buckling can also occur.

It was observed that for an initial imperfection of less than Length/1000, the shape of the imperfection has a relatively small effect. However, as the imperfection magnitude is increased, a more significant variation in results can be observed. For a weakened column with an imperfection magnitude of Length/100 the failure load can decrease by up to 30% in comparison to a weakened column with an imperfection magnitude of Length/1000. Even though is this paper an imperfection of Length/1000 is used, for future work, and for the prediction of real structural behaviour, higher imperfection values in conjunction with multiple buckling modes should be considered.

4.3 Boundary Conditions

The FE column models developed in this work were pinned about the weak axis and fixed about the strong axis, replicating the behaviour of the bearing used during physical testing. Precautions were taken during the experimental setup to ensure that the boundary conditions could be simulated as close as possible to those assumed for the finite element analysis (FEA). The most suitable way to simulate this kind of support condition in Abaqus, is through the use of a rigid beam multi-point constraint (MPC) connection (Yuan 2004). The rigid beam MPC method provides a beam connection between the reference point (master node) and the rest of the surface nodes (slave nodes), coupling the three displacement degrees of freedom and the three rotation degrees of freedom of the slave nodes to the master node. The master node inherits the average stiffness of the slave nodes (Dassault Systèmes 2016; Smalberger 2014).

4.4 Material Modelling and Residual Stresses

Abaqus requires a uni-axial stress–strain curve to model the material properties of an element. A number of idealized stress–strain curve models can be used for steel such as the linear elastic model, elastic perfectly plastic model, bilinear model, multi-linear models, Ramberg–Osgood models and many others (Thi Thu Ho 2010). In this paper the multi-linear stress–strain model is used, with the measured engineering stresses presented in Table 1 above being converted to true stresses for Abaqus (Roylance 2006).

Residual stresses in hot-rolled sections are primarily caused by differential cooling during the manufacturing process. The magnitude and distribution of the residual stresses depends on factors such as the rolling temperature, cooling conditions, straightening procedures and material properties. According to Galambos (1998) residual stresses typically have a limited effect on the buckling strength of very slender columns, however, they do reduce the inelastic buckling

capacity of intermediate slenderness columns. In practice cuts are made with a flame torch, causing a redistribution of residual stresses in a column. During the literature review negligible data was found regarding the redistribution or the magnitude of the residual stresses that would be suitable for columns weakened with flame torches. Hence, in order to quantify the effect of the residual stresses on a weakened column further research is required, although it is not expected to have a significant influence on results obtained. Therefore, for this research project the effect of the residual stresses was not included in the FE models.

5 Results

5.1 Control Columns and Model Validation

In order to determine the influence of the double window cut and the triangular window cut a reference control column test was necessary. Control column tests were conducted for each of the 13 m long sections obtained for suppliers, from which all samples were cut, with cut lengths of 0.6 m (only for the IPE 160 to ensure local failure was obtained), 1.0, 1.4 and 1.9 m.

Figures 9, 10, 11 and 12 illustrate the axial failure loads (a) from experimental tests, (b) predicted by FE models developed in this work, and (c) calculated using design codes. To understand the influence of cuts the experimental results from the control, double window and triangular

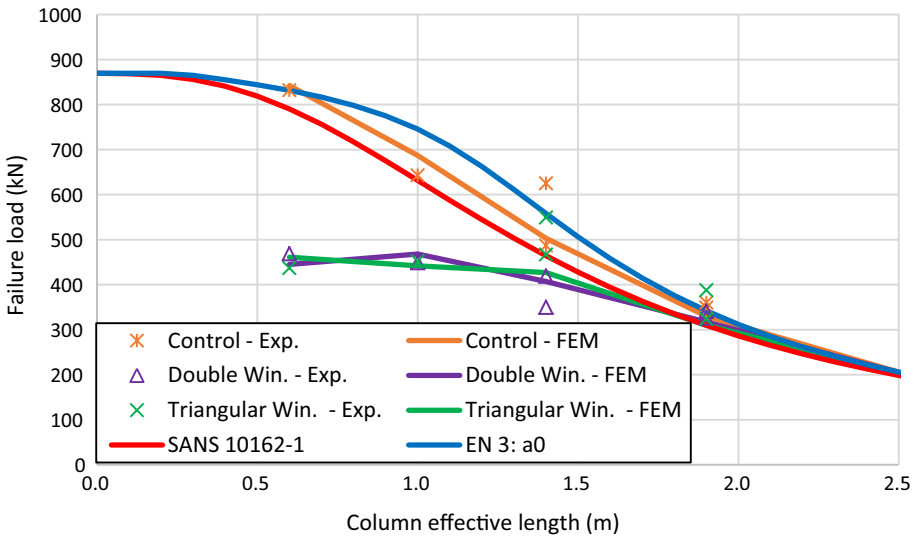

Fig. 9 Axial failure load of the IPE 160 control, double window and triangular window cut sections based on experimental results (Exp.), FE models (FEM) and design codes (SANS 10162-1 & EN 3-1-2)

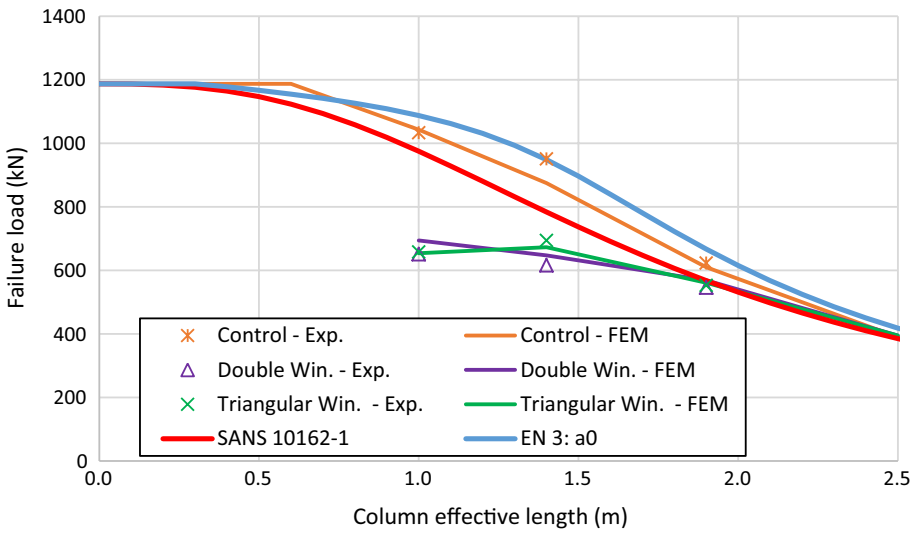

Fig. 10 Axial failure load of the IPE 200 control, double window and triangular window cut sections based on experimental results (Exp.), FE models (FEM) and design codes (SANS 10162-1 & EN 3-1-2)

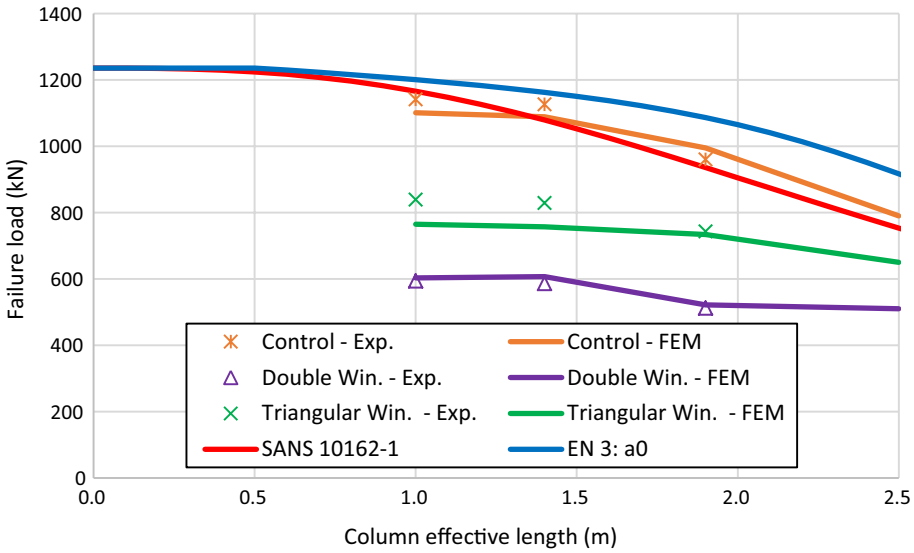

Fig. 11 Axial failure load of the UC 152 × 152 × 23 control, double window and triangular window cut based on experimental results (Exp.), FE models (FEM) and design codes (SANS 10162-1 & EN 3-1-2)

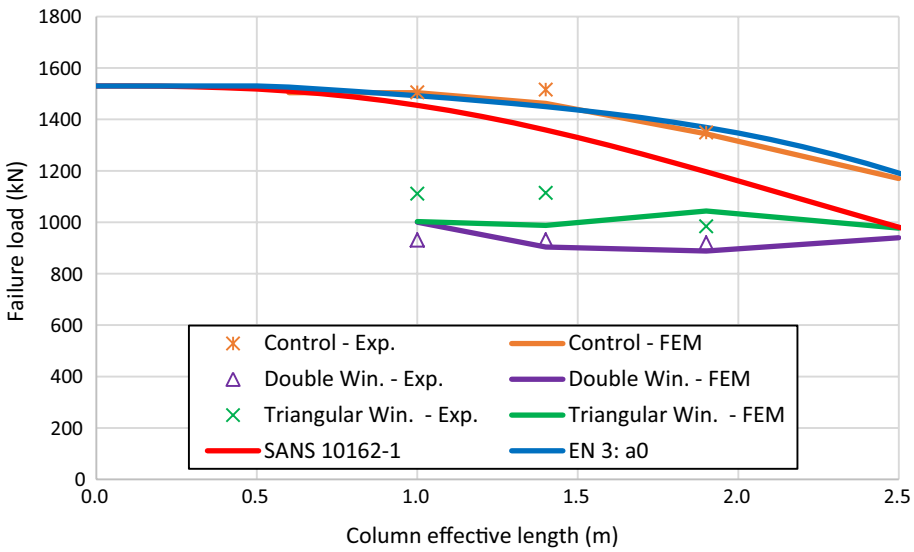

Fig. 12 Axial failure load of the UC 152 × 152 × 30 control, double window and triangular window cut sections based on experimental results (Exp.), FE models (FEM) and design codes (SANS 10162-1 & EN 3-1-2)

window cuts are shown on the same graphs for the four section sizes tested, but the weakened column results are discussed further in the sections that follow. The two design code curves considered are the South African design code, SANS 10162-1 (SABS 2011), and Eurocode EN 1993-1-1 (referred to as EN 3) (BSI 2014). The application of, and differences between, these two codes is discussed by Walls and Viljoen (2016). The failure loads calculated by these codes are included to show how initially the cuts reduce the capacity of the columns, but as slenderness ratios increase, and global buckling becomes more dominant, the behaviour of the weakened column tends towards that predicted by traditional design codes. Note that material factors have not been included in these calculations as material properties are accurately known.

From Figs. 9, 10, 11 and 12 it can be seen that the control test results for the four sections show good correlation with the FE models. The predicted FE model results differed by less than 8% from the experimental results. An outlier appears to be the one 1.4 m long test for the IPE 160 column, where a failure load of 625 kN was obtained. A second test done on the same section produced a failure load of 457 kN. During testing of the original sample was observed that either due to an alignment or bearing setup issue the bearing did not behave as fully pinned. As a precaution, all the IPE 160 tests on 1.4 and 1.9 m samples (for both the control and cuts) were done a second time, to ensure that accurate results were obtained. All results are presented below.

For the control tests the predicted failure stress for the SANS 10162-1 curve is consistently lower that the

experimental and FE model results. However, failure stresses predicted by EN 1993-1-1 show good agreement in comparison to the experimental results. The EN 1993-1-1 code has five buckling curves, with each curve associated with different levels of imperfection. In this work the EN 3 a_0 curve has been selected as it has a low level of imperfection, comparable to that measured in experiments. For application in practice a different design curve with a higher level of imperfection should be considered when demolition work is carried out.

Figure 13 illustrates the failure process of a 152 × 152 × 30 control section. It can be seen that the FE models accurately predict the failure behaviour of the control column in comparison to the experimental results, as shown in Fig. 13d. The axial stress is indicated for the FE models. Figure 13c indicates that yielding occurred at the inside of the column due to compression (blue) and the outside due to tension (red), and this was also observed during the experiments where the whitewash would crack due to flaking of mill scale. Such behaviour should be considered when viewing the weakened columns shown in the following sections.

5.2 Double Window Cut

Table 2 presents the experimental and predicted FE compressive failure loads for the specimens tested with the double window cuts, with results being shown in Figs. 9, 10, 11 and 12. In general, it can be seen that there is good agreement with differences being less than 8%. The variation in results is due to factors such as the variation in cross-sectional dimensions from perfect specified values, the influence of imperfections, residual stresses, potential variations in material properties and other such factors. For the 1.9 m long IPE 160 sample global buckling becomes the dominant failure mode, and the cut has a significantly

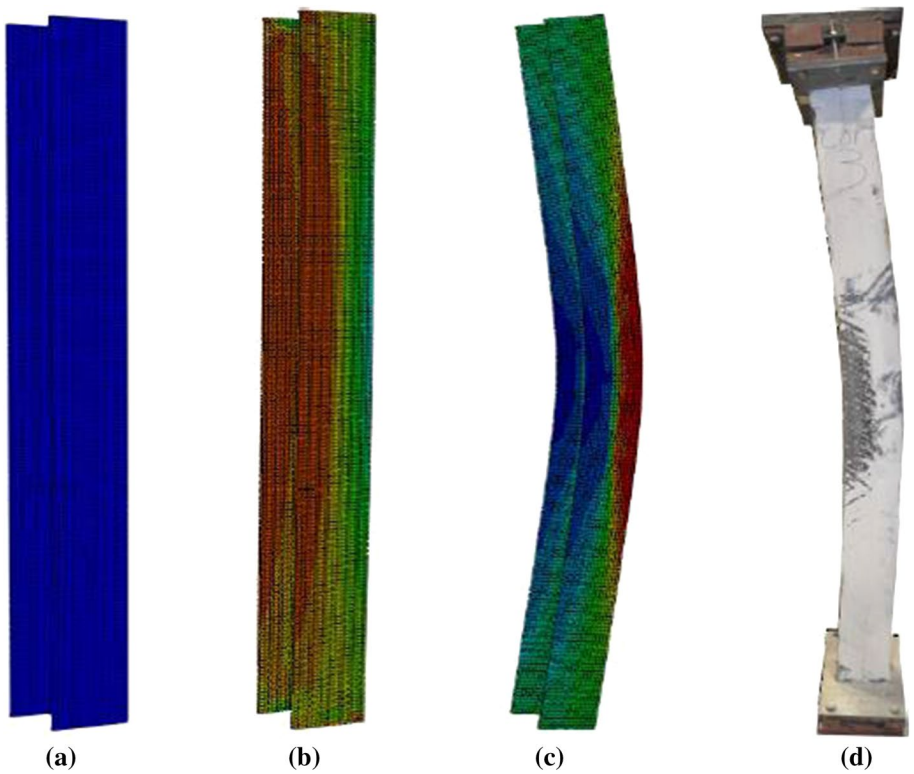

Fig. 13 Buckling of 152 × 152 × 30 control section for FE models and experiment. **a** No axial load, **b** at critical load, **c** after failure, **d** experiment. (Color figure online)

Table 2 Experimental (exp.) and finite element (FE) failure loads (in kN) for the double window cut tests

Length (m)	IPE 160			IPE 200			UC 152 × 152 × 23			UC 152 × 152 × 30		
	Exp.	FE	% diff.	Exp.	FE	% Diff.	Exp.	FE	% diff.	Exp.	FE	% diff.
0.6	469	445	− 5.1									
1.0	449	468	4.2	651	694	6.6	594	603	1.5	931	1000	7.4
1.4	419 (350)	407	− 2.9	616	647	5.0	586	607	3.6	931	904	− 2.9
1.9	341/326	317	− 7.0/− 2.8	546	569	4.2	512	522	2.0	919	888	− 3.4

reduced influence on the failure load, in comparison to an uncut sample. For the 1.4 and 1.9 m long IPE 160 samples two tests were done to verify results, and it appears that for the one 1.4 m sample that an experimental error occurred (misalignment which reduced capacity).

From Figs. 9, 10, 11 and 12 it can be seen that the double window cut can reduce the capacity of a column by up to around 50%. After carrying out this calibration exercise for FE models, additional models were created for columns with various lengths, in order to understand the behaviour of weakened columns over the entire slenderness ratio spectrum. From the additional data points it can be seen that the double window cut influences the compression failure stress significantly up to a slenderness ratio of around 85. For higher slenderness ratios global buckling becomes dominant, and thus the influence of the cut becomes significantly reduced. The behaviour of all the columns is similar to that shown for the IPE 160 in Fig. 9 (which covers the short to slender range), where FE and code predictions converge at higher slendernesses, meaning that the cut has only a limited effect on the capacity. The 1.9 m long IPE 160 specimens tested clearly shows global buckling to be the dominant mode of failure. Failure modes are discussed further in Sect. 5.4 below.

From Figs. 9, 10, 11 and 12 it can be observed that the results obtained from the FE models do not indicate a constant compression failure load for slendernesses at which experimental data is shown. This is due to the fact that the three FE models correspond to the actual dimensions and yield stress of the tested sections. For the additional FE models the properties correspond to the dimensions of the template, and the average yield stresses, as shown in Table 1. The results obtained from the FE models and experiments indicate that there is only a slight decrease in the compression failure load relative to an un-weakened column as the slenderness of the column increases. Figure 14 illustrates the failure process of a UC 152 × 152 × 30 with a double window cut which is as follows:

(a) The initial column, without any axial load applied.
(b) The point at which buckling occurs in the column.
(c) The column after buckling occurred.

The FE models could accurately predict the failure behaviour of the double window cut, as compared to the experimental results in Fig. 14d. From Fig. 14b it can be seen that due to the small amount of eccentricity, the sub-column starts to buckle causing hinges at the ends on the sub columns. The areas where the material yields can be visually identified in experiments from the positions where the whitewash has cracked due to flaking of mill scale, as seen in Fig. 14d. This corresponds to the FE model stress distribution, which are indicated by the red (tension) and blue (compression) areas.

Throughout the FE model analysis it was observed that the cut in the web remains open. This behaviour was observed for all the experiments that were conducted. This

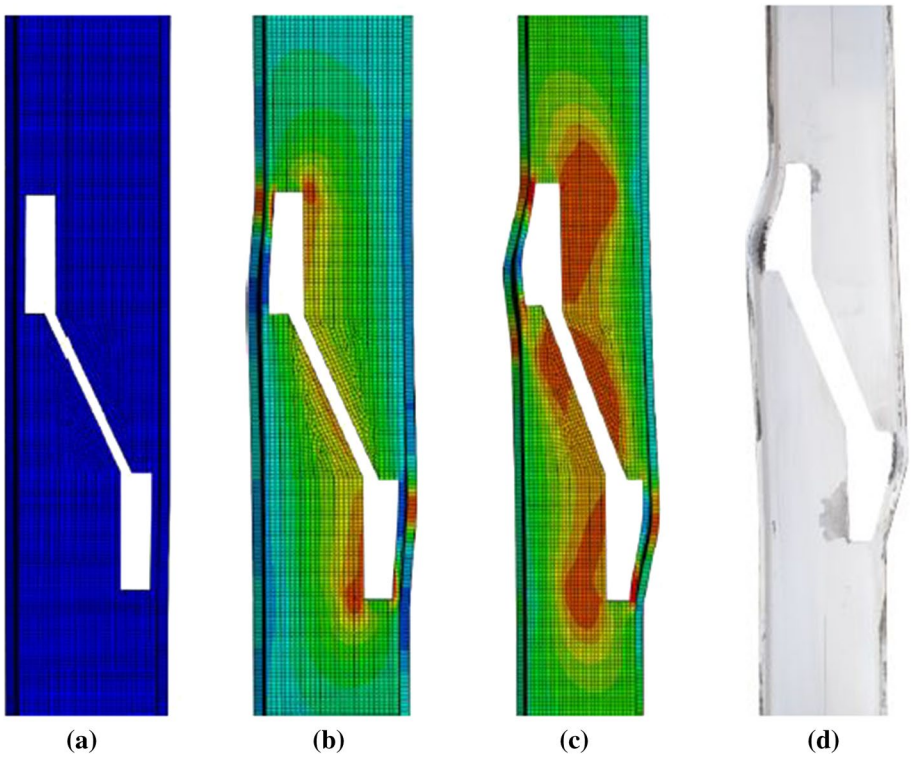

Fig. 14 Buckling of a 152 × 152 × 30 section with a double window cut showing FE models and experimental results. **a** No axial load, **b** at critical load, **c** after failure, **d** experiment. (Color figure online)

indicates that the diagonal cut is necessary for the section to freely displace to the side causing a P-Δ effect and a change in the effective length of the sub-column. It also can be seen that the failure of the overall column was due to the buckling of the two sub-columns. The plastic–elastic hinges that form in each of the corners can also be observed.

5.3 Triangular Window Cut

Table 3 compares the experimental and finite element failure loads for the various member sizes and lengths tested with the triangular window cut. In general, there is good agreement between results, with predicted results being less than 10% different from experimental results, except for the UC 152 × 152 × 30 at 1.4 m in length which is at − 11.3%. Factors influencing this variation in results are discussed in Sect. 5.2 above. However, it is interesting to note that FE results are typically lower than experimental results. Potentially a lower imperfection value could be used, or some form of localised strain-hardening may influence results. As mentioned above, it appears that the one result for the IPE 160 section at 1.9 m long was an outlier due to an experimental error.

Figures 9, 10, 11 and 12 indicate that the triangular window cut can reduce the capacity of a column by up to 40% (with the 0.6 m IPE 160 being 48%). The difference between the predicted FE model results and the experimental results is typically less than 10%, as discussed above. This is within an acceptable level of accuracy when the high level of uncertainty inherent in demolition, such as the material properties, initial geometric imperfection and the redistribution of the residual stresses is considered.

Similar to the double window cut, additional models were created with various lengths in order to obtain the behaviour of the weakened column over the entire slenderness ratio range, as presented in the aforementioned figures. Additional FE column models that were created and analysed, and as per the double window cut predicted capacities converge on those determined by design codes for unweakened sections. Where data has been extrapolated the dimensions of the cutting template and the average yield stresses according to Table 1 were used.

Table 3 Experimental (exp.) and finite element (FE) failure loads (in kN) for the triangular window cut

Length (m)	IPE 160			IPE 200			UC 152 × 152 × 23			UC 152 × 152 × 30		
	Exp.	FE	% diff.	Exp.	FE	% diff.	Exp.	FE	% diff.	Exp.	FE	% diff.
0.6	437	461	5.5									
1.0	452	442	− 2.2	658	654	− 0.6	839	765	− 8.8	1111	1003	− 9.7
1.4	459/467	433	− 5.7/7.3	698	673	− 3.6	829	757	− 8.7	1114	988	− 11.3
1.9	324 (388)	306	− 5.6	553	561	1.4	743	734	− 1.2	984	1044	6.1

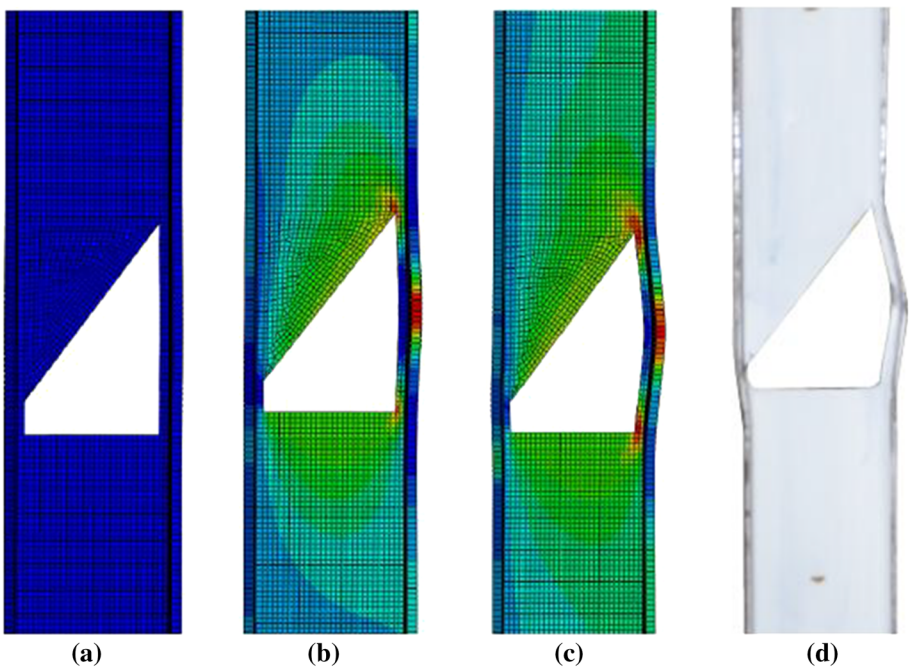

Fig. 15 Buckling of a 152 × 152 × 30 section with a triangular window cut showing FE models and experimental results. **a** No axial load, **b** at critical load, **c** after failure, **d** experiment. (Color figure online)

Figure 15 illustrates the failure process of an IPE200 triangular window cut which is as follows:

(a) The initial column, without any axial load applied.
(b) The point at which buckling occurs in the column.
(c) The column after buckling occurred.

It can be seen that the FE models accurately predict the failure behaviour of the triangular window cut when compared to the experimental results. From Fig. 15 it can be understood that initially (1) the sub-column buckles, and (2) hinges start to form in the ends and in the middle of the sub-column. Similar to the double window cut, Fig. 15d shows the areas of material yielding where the whitewash has cracked in the experiment. This corresponds well to the FE models, which are indicated by the red (tension) and blue (compression) areas. The plastic–elastic hinges that form in each of the corners and in the middle of the longer sub-column can also be observed.

5.4 Consideration of Failure Behaviour

From the results presented above it can be seen that there are two predominant failure modes for weakened columns, namely: (a) a sub-column localised failure mode at low slendernesses, evidenced by a plateau on the compression failure graphs, and (b) a global buckling mode similar to that predicted by contemporary design codes. The failure plateau is in the order of 40–50% below the capacity of the un-weakened column, although this is strongly influenced by the size and shape of the cut made. Hence, with additional research work it is hypothesised that it will be possible to characterise the full structural response of weakened columns by developing localised sub-column failure equations, coupled with existing design equations.

5.5 Consideration of Cut Geometry

As discussed in Sect. 2, the geometry of a cut has an influence on the capacity of the column. A parametric investigation has been carried out to investigate the influence of changing design properties. If global buckling dominates failure then cut geometry has negligible influence, but when local sub-column failure governs then cut geometry becomes more important. Sub-columns buckle as small T-shaped columns, so changes in the following will influence capacity: effective length, cross-sectional area, and radius of gyration about the T-section's weakest axis.

For the double window cut the following specific parameters have been considered:

- Length of vertical cut section: Since the sub-columns experience compressive buckling failure an increase in the length of the vertical cut decreases the column capacity, as discussed above. If the cut is varied from 100 to 300 mm the capacity can decrease by up to 33%, depending on column geometry.
- Angle of cut: When the cut angle was varied from 17° to 60° it was found that it has a negligible influence on capacity, provided that the rectangular window dimensions remain constant.

For the triangular window cut the height of the cut and resultant cross-sectional T-section properties are the dominant factors influencing behaviour. Capacity reduces with increasing height of cut in a manner similar to that predicted by hot-rolled steel codes for columns (e.g. BSI 2014).

6 Conclusion

To date, the capacity of columns weakened to facilitate the demolition of buildings has typically been determined only by experience obtained from previous projects, and has generally not been focused on strict theoretical principles. This has great implications for safety, such as buildings collapsing during the weakening process. This paper provides a detailed set of experimental results which show the behaviour of columns weakened using a triangular window or double window cut. This has been done to improve understanding regarding such structural behaviour and to provide data for developing analysis models, thereby improving safety and efficiency during the demolition process. A finite element model was developed based on the results obtained. This model could be used to predict failure loads prior to demolition teams working on structures, such that safety can be ensured.

The effect of an initial geometric imperfection on the axial load capacity is important to consider. A sensitivity study highlighted that the load capacity is dependent on the imperfection factor and its magnitude. Significantly larger imperfection factors than the value of Length/1000 should be used for FE models when predicting failure loads in real structures, although the aforementioned value was used in this based paper based on experimental measurements and tolerances.

The test results obtained for the control columns agreed well with the FE models. The differences were typically less than 8–10%. The results obtained for the double window cut indicate that the capacity of a column may be reduced by up to 50%, whilst for a triangular window cut this in the order of 40%. The extrapolated data points indicate that the capacity of a column is not significantly influenced by the presence of a cut once global buckling governs. This transition from local to global buckling occurs at a slenderness ratio of around 85, depending on column size and cut geometry.

Based on the discussions above it can be understood that the failure of weakened columns can be considered as being governed by two distinct failure modes. At low slendernesses local sub-column buckling governs, which presents as a maximum load plateau on the load versus slenderness graphs. At higher slenderness ratios global buckling governs failure, and the capacity is reduced less than might be expected due to the presence of a cut. Future work will focus on developing simplified hand calculation methods to predict the failure of columns without requiring the use of FE software. This will be of significant benefit to those involved in the demolition engineering field.

Acknowledgements This work has been supported in part by the Wilhelm Frank Foundation and the National Research Foundation of South Africa under a Thuthuka Grant, Unique Grant No. 99304. Any opinion, finding and conclusion or recommendation expressed in this material is that of the author(s) and the funders do not accept any liability in this regard.

References

Avery, P., & Mahendran, M. (2000). Distributed plasticity analysis of steel frame structures comprising non-compact sections. *Engineering Structures, 22*(8), 901–919.

BSI. (2014). *BS EN 1993-1-1:2005 + A1:2014—Eurocode 3: Design of steel structures—Part 1-1: General rules and rules for buildings, Eurocode 3, Amd. 1*. London: British Standards Institute.

Chabrolin, B. (2001). *Partial safety factors for resistance of steel elements to EC3 & EC4. Calibration for various steel products and failure criteria*, Final report. St-Rémy-lès-Chevreuse: Centre Technique Industriel de la Construction Métallique (CTICM).

Dassault Systèmes. (2014). *Abaqus analysis user's manual. Abaqus 6.14.1*. Vélizy-Villacoublay, France: Dassault Systèmes Simulia Corporation.

Dassault Systèmes. (2016). *Abaqus*. Providence, RI: Dassault Systèmes.

Dunn, T. (2015). *Demolition engineering: Analysis, testing and design of weakened steel columns prior to collapse*. Stellenbosch: Stellenbosch University.

Estuar, F. R., & Tall, L. (1967). *The testing of pinned-end columns*. Tech. rep. 1683. Lehigh University Institute of Research.

Galambos, T. V. (1998). *Guide to stability design criteria for metal structures* (5th ed.). New York: Wiley. http://books.google.com/books?hl=es&lr=&id=W_a0-8wiHdwC&pgis=1.

HK Bldg. Dept. (2004). *Code of practice for demolition of buildings*. Hong Kong, PRC: Hong Kong Buildings Department.

IS. (2002). *IS 4130 (1991): Safety code for demolition of buildings [CED 29: Construction management including safety in construction]*. New Delhi: Bureau of Indian Standards.

JISF. (2015). Demolition of high-rise buildings and bridges. *Steel Construction Today & Tomorrow, April*(44), 7–13.

Mitchell, D. (2016). *Demolition engineering: Lateral load carrying capacity of weakened steel beams*. Stellenbosch: Stellenbosch University.

NDA. (2014). FAQs about demolition. *National Demolition Association Webpage*. http://www.demolitionassociation.com/demolition-faq. Accessed 1 Nov 2015.

Roylance, D. (2006). *Stress–strain curves* (Vol. 3). Cambridge: Massachusetts Institute of Technology.

SABS. (2005). *SABS 2001:CS1 (2005)—Construction Works-Part CS1: Structural Steelwork* (1st ed.). edited by South Afrucan Bureau of Standards, Pretoria.

SABS. (2010). *SABS 6892-1 (2010). Metallic materials-tensile testing. Part 1: Method of test at room temperature* (1st ed.). Pretoria: South African Bureau of Standards.

SABS. (2011). *SANS 10162-1: 2011 South African National Standard the structural use of steel part 1: Limit-states design of hot-rolled steelwork*. Pretoria: SABS.

Smalberger, H. J. W. (2014). *Comparative study of the equivalent moment factor between international steel design specifications*. Stellenbosch: Stellenbosch University.

Tebedge, N., Marek, P., & Tall, L. (1971). *On testing methods for heavy columns*. Tech. rep. 351.4. Lehigh University Institute of Research.

Thi Thu Ho, C. (2010). *Analysis of thermally induced forces in steel columns subjected to fires*. Texas, USA: University of Texas at Austin.

van Helsdingen, G. C. F. (2012). *Investigation into the load capacity of weakened columns*. Pretoria: University of Pretoria.

van Jaarsveldt, W. J. (2016). *Predicting the failure load of steel columns weakened to facilitate demolition of structures*. Stellenbosch: Stellenbosch University.

van Jaarsveldt, W. J., & Walls, R. S. (2016). Predicting the failure load of steel columns weakened to facilitate demolition of a structure. In A. Zingoni (Ed.), *Insights and innovations in structural engineering, mechanics and computation* (pp. 1190–1195). Cape Town: Taylor & Francis.

Walls, R. S. (2017). Demolition of steel structures: Structural engineering solutions for a more sustainable construction industry. In Y. Bahei-El-Din & M. Hassan (Eds.), *Advanced technologies for sustainable systems* (pp. 3–8). Cairo: Springer.

Walls, R. S., & Viljoen, C. (2016). A comparison of technical and practical aspects of Eurocode 3-1-1 and SANS 10162-1 hot-rolled steelwork design codes. *Journal of the South African Institution of Civil Engineering, 58*(1), 16–25.

Yuan, Z. (2004). *Advanced analysis of steel frame structures subjected to lateral torsional buckling effects*. Brisbane: Queensland University of Technology.